LAL 04-20
hep-ph/0406010
LC-PHSM-2004-016
May 2004

Experimental Implications for a Linear Collider of the SUSY Dark Matter Scenario

P. Bambade[a], M. Berggren[b], F. Richard[a], Z. Zhang[a,1]

[a]**Laboratoire de l'Accélérateur Linéaire,**
IN2P3-CNRS et Université de Paris-Sud, Bât. 200, BP 34, 91898 Orsay Cedex, France

[b]**Laboratoire de Physique Nucléaire et de Hautes Energies,**
IN2P3-CNRS et Université Paris VI-VII, 4 place Jussieu, Tour 33 - Rez de chaussée, 75252 Paris Cedex 05, France

Work presented at the International Conference on Linear Colliders (LCWS04) 19-23 April 2004, "Le Carré des Sciences", Paris, France

Abstract

This paper presents the detection issues for the lightest slepton $\tilde{\tau}_1$ at a future e^+e^- TeV collider given the dark matter constraints set on the SUSY mass spectrum by the WMAP results. It intends to illustrate the importance of an optimal detection of energetic electrons in the very forward region for an efficient rejection of the $\gamma\gamma$ background. The TESLA parameters have been used in the case of head-on collisions and in the case of a 10 mrad half crossing angle.

[1]E-mail: bambade@lal.in2p3.fr, mikael.berggren@cern.ch, richard@lal.in2p3.fr, zhangzq@lal.in2p3.fr

1 Introduction

The present paper is motivated by the increasing awareness in the community of the role of an e^+e^- Linear Collider (LC) for a precise determination of the SUSY parameters which are needed to interpret the dark matter (DM) content of the universe. After the WMAP results leading to an accuracy on $\Omega_{\rm DM}h^2$ at the 10% level and awaiting for the Planck mission in 2007 which aims at 2%, it seems appropriate to check that a LC can do its job properly on this essential topic. The main issue is to compare the SUSY prediction derived from the collider measurement and the DM result observed in our universe. A significant mismatch would reveal the existence of extra components of DM in the universe which are predicted within SUSY (e.g. the gravitinos) or beyond SUSY (e.g. the axions).

An important issue is also to check with this type of physics the effect of some choices discussed for the future LC. This paper will explain in which way the DM issue can provide some useful informations. After an introduction of these arguments intended for 'pedestrians', a quantitative study will be presented to illustrate the problem.

In the SUSY scenario with R-Parity conservation, the lightest SUSY particle (LSP) is the lightest neutralino χ. This particle is considered as the best candidate to satisfy the cosmological constraints on DM in the universe. DM constraints have been recently re-examined [1] within the mSUGRA scenario, confronting the precise predictions obtained after the WMAP results. These data imply, for many of the working points retained, a very small difference between the lightest slepton mass, the SUSY partner of the τ which will be called $\tilde{\tau}_1$, and the LSP mass since one of the preferred mechanism to regulate the amount of DM in the universe is the so-called 'co-annihilation mechanism'. Since this feature is quite general and goes beyond the mSUGRA scheme as pointed out in [2], one should investigate the possible experimental consequences on the detection of sleptons at a LC. The detectability of the tau slepton in such a small mass difference has been discussed recently in [3] in mSUGRA for a 500 GeV LC collider.

To understand the effect of mass degeneracy, one should recall the mechanism which regulates the amount of DM in the universe and is based on thermodynamics and on annihilation cross sections between SUSY particles. The $\chi\chi$ annihilation cross section is small since it occurs in a p-wave (Fermi exclusion principle for identical fermions) with a kinematic suppression at threshold. A way out is to annihilate χ with $\tilde{\tau}_1$ but, given the Boltzmann law, this can only occur during the cooling of the early universe if these particles have a small mass difference. How small should this mass difference be? Typically the ratio between the stau and neutralino populations is given by $\exp(-\Delta m/T_f)$ where Δm is the mass difference and where T_f is the freeze-out temperature which is $\sim m/20$. To avoid a strong depopulation of $\tilde{\tau}_1$, the mass difference should therefore be below $m/20$ which in practice means typically below 10 GeV. Since $\tilde{\tau}_1$ is significantly lighter than the other sleptons, the amount of DM will therefore primarily depend on the mass difference between χ and $\tilde{\tau}_1$ masses. When the χ mass increases one needs to increase the annihilation efficiency to keep at the same level the amount of DM density in the universe. This means that one needs to reduce even further Δm. When the neutralino mass reaches about 500 GeV this mechanism does not work anymore which gives an important upper limit on SUSY particles.

Admittedly there are other ways to solve this problem as will be discussed in detail in the next section.

From this qualitative presentation, one therefore concludes that the SUSY scenario implies that:

1. the mass difference between $\tilde{\tau}_1$ and the LSP is likely to be below 10 GeV,

2. the amount of DM depends critically on the mass of the stau particle.

Experimentally this means that the stau channel should be cleanly detected to measure its mass through a threshold scan. Near threshold, the cross section is at the 10 fb level with a potentially very large background due to the four fermion final states, the so-called '$\gamma\gamma$' background, which is at the nb level. Moreover $\tilde{\tau}_1$ decays into a τ lepton with one or two neutrinos in the final state which even further reduces the amount of visible energy.

In usual cases the standard backgrounds can be eliminated by requiring that the two observed leptons be acoplanar thus eliminating the $\gamma\gamma$ background provided that the forward veto forces spectator electrons to be emitted at almost zero angle in the four fermion process. This veto usually starts above a polar angle of 5 mrad which is sufficient to cope with ordinary SUSY mass differences for a 500 GeV collider. The present paper intends to quantify the effect for the SUSY solutions retained in [1].

The next issue to be considered is the reduction in efficiency of this veto in case there is a crossing angle between electron and positron beams, ± 10 mrad, as needed in the warm technology and as also envisaged in the TESLA scheme.

Finally, one should also worry about the efficiency of this veto given the very large overlaid background produced by beam-beam interaction which hits the very forward electromagnetic calorimeter. This paper therefore also intends to provide an input on these various aspects.

2 DM and SUSY

For a simple discussion of the issues presented in the introduction, the mSUGRA scheme is hereafter adopted. The mass spectrum depends on two parameters $m0$ and $M1/2$, the common masses of scalars and gauginos superpartners at the unification scale. The parameter μ, defining the higgsino mass, is derived, in absolute value, by imposing the electroweak symmetry breaking (EWSB) condition in terms of these two parameters and of $\tan\beta$, the ratio of the vacuum expectations which appear in the two Higgs doublets of SUSY. The various regions allowed by EWSB and DM constraints and the position of the various working points chosen are schematically displayed in figure 1.

1. For moderate values of $m0$ and $M1/2$, the LSP solution is a Bino, the SUSY partner of the SM $U(1)$ gauge boson. The annihilation cross section for a pair of LSP, which controls the amount of DM in the universe, proceeds through selectron exchange and can be easily adjusted to cope with the WMAP constraints.

2. For larger values of $M1/2$ and moderate values of $m0$, the rate of annihilation through selectron exchange becomes insufficient and co-annihilation between the LSP and the lightest sleptons, in particular $\tilde{\tau}_1$, are needed. When the LSP mass increases, the co-annihilation process should increase, meaning that the mass difference between the LSP and the slepton should tend to zero at some point. For moderate values of $\tan\beta$ (not larger than 30), this maximum value is about 500 GeV, which incidentally means that this type of mechanism for generating DM should be covered by a TeV collider. The exact amount of DM in the universe depends crucially on the mass of the LSP, which can be easily determined using end-points smuon (or selectron) decays as can be seen in figure 7, and on the mass of $\tilde{\tau}_1$ which

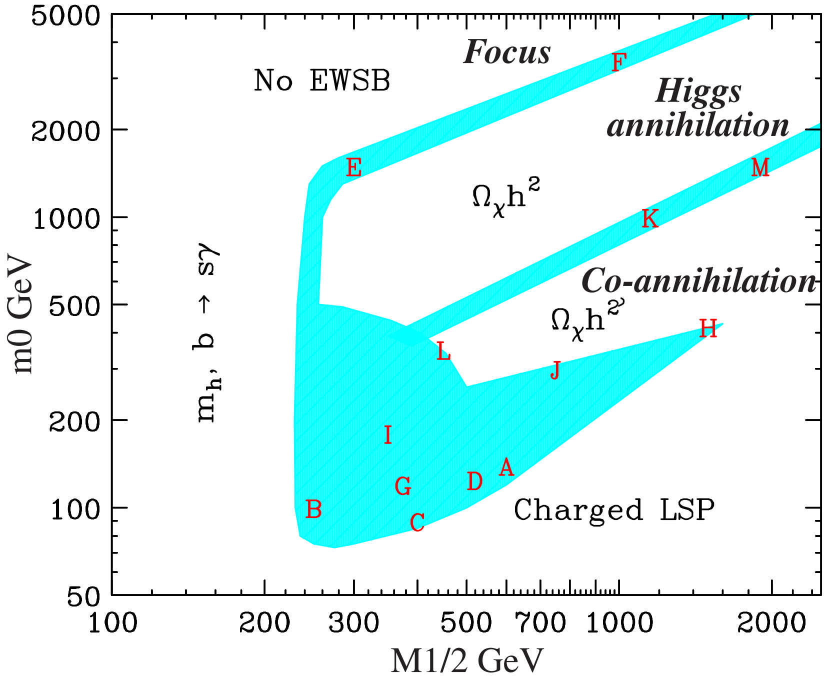

Figure 1: *Schematic view of the various DM solutions described in the text and display of the various working points proposed in [1].*

can be determined through a threshold scan.[2] If the mass difference between the lightest stau and the LSP is too small, the separation from the background will become problematic and these scans could be extremely time consuming or even impossible. The accuracy on the $\tilde{\tau}_1$ mass is primordial since it governs the accuracy on the prediction of DM in the universe which will be known to a few percent after the Planck mission. This aspect will therefore be the main emphasis of the present study.

3. For large values of $m0$ and $M1/2$ there are, within mSUGRA, two scenarios to cope with the WMAP constraints.

   In the 'focus' solution, $m0$ is large but μ can be smaller than $M1/2$ meaning that the LSP is of the higgsino type and therefore can annihilate into WW/ZZ pairs in the early universe. This solution can lead to a degeneracy between the LSP and the lightest chargino but, given that the chargino cross section is much larger than the slepton one, this situation can be dealt with using events having photons originating from initial state radiation (ISR) as was shown at LEP2. It turns out, however, as will be discussed in section 7.3, that the degree of degeneracy is not severe for light neutralinos and therefore one can achieve standard accuracies for light gaugino masses. As pointed out in reference [4] and as can be seen in figure 2,[3]

[2] An alternative approach would be to analyze the high energy spectrum. This method however requires that the stau mass is relatively small with respect to the beam energy and the signal production cross section is large enough in comparison with background contributions in the final energy spectrum.

[3] This is a modified version of figure 8 from reference [4] by exchanging the x and y axes so that they

this type of solution is not well covered by LHC since, with very heavy squarks and gluinos, the only accessible SUSY particles are the first generation chargino and the two lightest neutralinos which need to be produced directly through quark-antiquark annihilation.

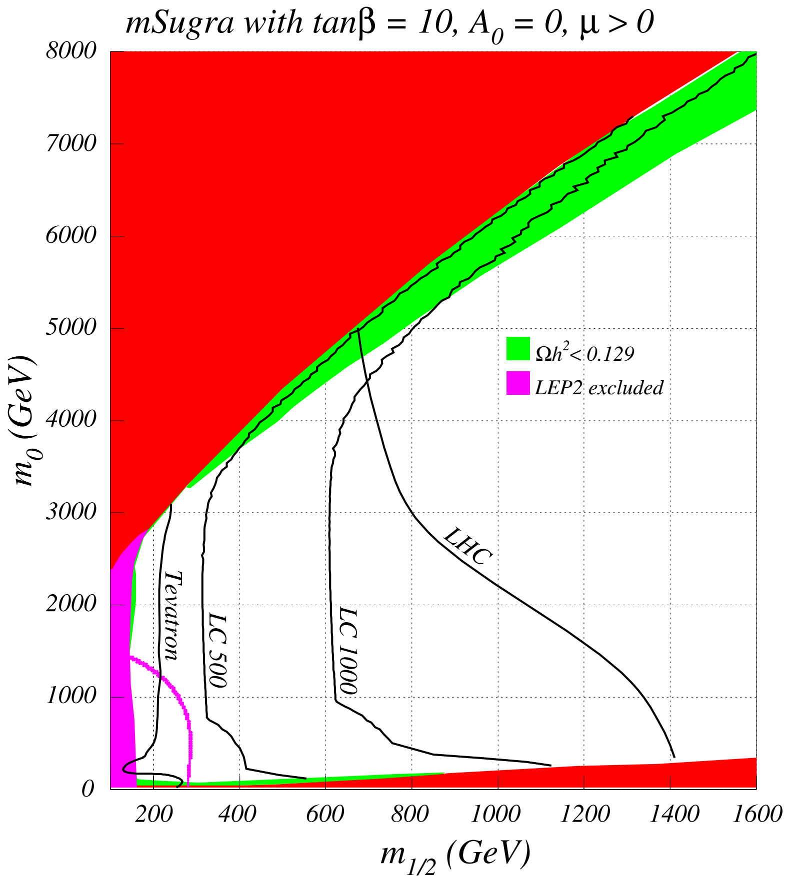

Figure 2: *A modified version of figure 8 from reference [4] showing the allowed DM solutions in green in the mSUGRA scheme for* $\tan\beta = 10$ *and* $\mu > 0$*. The regions to the left of the black curves are the domain covered by LHC and a LC at* 500 *and* 1000 GeV *respectively for an integrated luminosity of* $100\,fb^{-1}$ ($10\,fb^{-1}$ *for the Tevatron).*

In the 'Higgs annihilation' solution, the LSP mass is close to half the heavy CP odd Higgs mass meaning that LSP annihilate through $s-$channel into a heavy Higgs. This mechanism only operates for very large values of $\tan\beta$, typically above 40, which are allowed and even needed to accomplish unification between the Yukawa couplings of the third generation (but discarded in some 'string inspired' theories [5]). This solution leads to no particular constraints on the detection of the LSP but corresponds to mass solution which tends to fall beyond the reach of LC and, in some cases, even also beyond the reach of LHC.

Figure 2 shows, for moderate $\tan\beta$, the allowed region in green and the expected coverage from LHC and LC. In the co-annihilation region, at moderate $m0$, the LHC has a wider

are the same as in figures 1 and 3.

coverage but the LC can fully cover the DM solutions provided that there are no detection problems. In the focus region, LC extends the reach of LHC but, as previously mentioned, the detection issue is less critical and will be briefly discussed in section 7.3.

The $g-2$ measurement [6] indicates a deviation with respect to the SM prediction based on e^+e^- data. The deviation favors $\mu > 0$ and moderate mSUGRA masses. The indication is confirmed since the e^+e^- CMD2 data used are found in good agreement with the recent data [7] of KLOE based on the radiative return method. The discrepancy [8] with the τ decay analysis from LEP1 and CLEO, which is significant, remains however to be clarified.

Figure 3 from [9] indicates that, taking into account the old $g-2$ constraint, the most likely solutions correspond to the co-annihilation region. With the recent update from BNL [6], the deviation with respect to the e^+e^- SM prediction, is almost reaching 3 standard deviations (s.d.) and should therefore increase the significance of this indication.

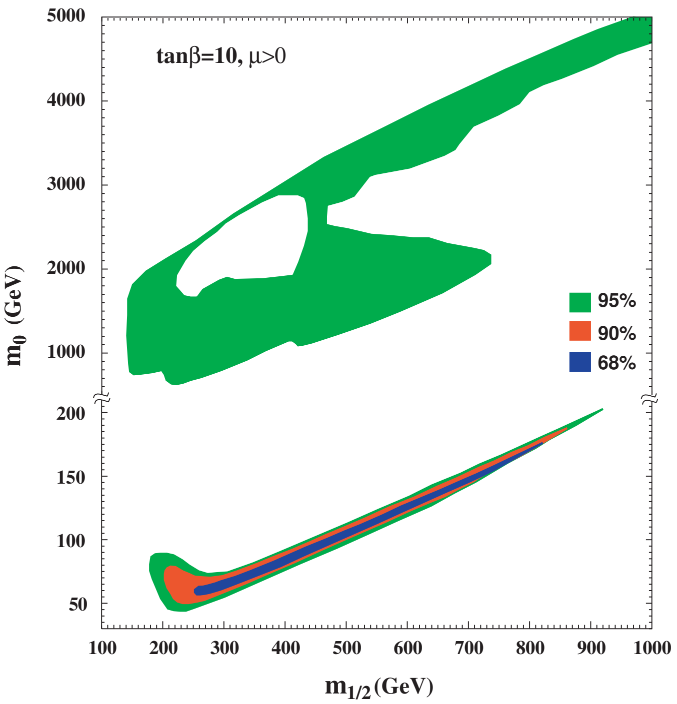

Figure 3: *For* $\tan\beta = 10$ *and* $\mu > 0$, *the acceptable mSUGRA solutions [9] are shown respecting the various constraints including the* $g-2$ *results. The most likely region, with* 68% *likelihood, corresponds to the co-annihilation region.*

There are several caveats to above conclusions. First, the co-annihilation solution may sound heavily 'fine tuned' since it requires a very tight correlation between the two mSUGRA mass parameters. One can however notice that in the so called 'gaugino mediated SUSY breaking' scenario, $m0$ which is loop-mediated is naturally small and a mass degeneracy between the neutralino and the right-handed sleptons occurs naturally [10]. The two other mechanisms previously discussed are also fine tuned and one cannot really object to any of these solutions in the absence of a definite SUSY breaking scheme. One may also argue that, in a general MSSM scheme, there is more flexibility and one could for instance have a wino-like LSP, in which case there is no need for the co-annihilation mechanism to regulate primordial DM. In this general MSSM approach and for other phenomenological reasons (e.g. CP violation in the flavor sector, proton lifetime constraints) one may wish to have very heavy sleptons at least for the first two generations. In this case the LSP mass could not be anymore determined from the smuon analysis but would require to use the chargino/neutralino channels. There could however still be a similar experimental problem, with co-annihilation between the stau and the neutralino with small mass difference.

Table 1 recalls the mSUGRA solutions retained in [1] and clearly indicates the trend described above. Figure 7 shows the energy distribution of the muons originating from smuon decays for solution D′. Two end points are clearly visible and their measurement allows to precisely extract the values of the mass of the slepton and of the LSP provided the lower point can be separated from the $\gamma\gamma$ background. The serious concern is about the stau analysis which, as shown in the same figure, has very soft final state particles to deal with.

Table 1: *Working points (model) taken from reference [1]. Note that in some cases (E′,F′,H′,M′) the resulting DM content obtained from Micromegas [17] does not match the WMAP constraints.*

Model	A′	B′	C′	D′	E′	F′	G′	H′	I′	J′	K′	L′	M′
$M1/2$	600	250	400	525	300	1000	375	935	350	750	1300	450	1840
$m0$	107	57	80	101	1532	3440	113	244	181	299	1001	303	1125
$\tan\beta$	5	10	10	10	10	10	20	20	35	35	46	47	51
$\mu(m_Z)$	773	339	519	-663	217	606	485	1092	452	891	-1420	563	1940
m_χ	242	95	158	212	112	421	148	388	138	309	554	181	794
m_{e_R}	251	117	174	224	1534	3454	185	426	227	410	1109	348	1312
m_{τ_1}	249	109	167	217	1521	3427	157	391	150	312	896	194	796
Δm	7	14	9	5	1409	3006	9	3	12	3	342	13	2
$\Omega_{\rm DM}h^2$	0.09	0.12	0.12	0.09	0.33	2.56	0.12	0.16	0.12	0.08	0.12	0.11	0.27

3 Forward set-up used to veto electrons

A detailed description of the forward equipment used in TESLA can be found in the TDR [11] and is shown in figure 4. The most relevant calorimeter for the present study is the LCAL, used as a beam monitor. In the TDR, this detector was situated at 2.6 m and started at $R = 1.2$ cm. In a recent upgrade of the final focus set up, the final quadrupoles have been moved downstream in such a way that the calorimeter is now at 3.7 m, at the same radius therefore covering an angle down to 3.2 mrad.

The energy density distribution of the background induced by beam-beam interactions is given in figure 5. This distribution corresponds to one bunch crossing since in the TESLA configuration the calorimeter can be read before the next crossing. The detection of energetic electrons is possible everywhere since these electrons can be recognized from the low energy electrons which dominate the background using the longitudinal energy profile of their shower. An optimal treatment of the vetoing procedure is still underway.

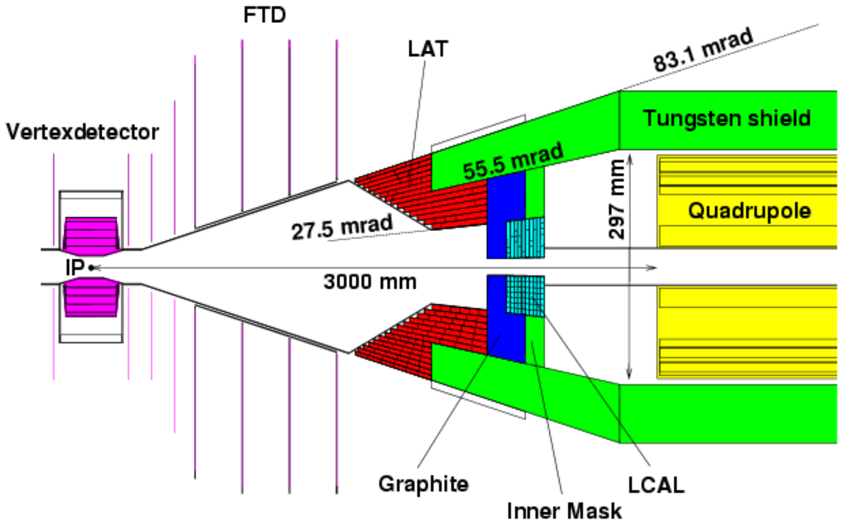

Figure 4: *Forward region given in the TDR of TESLA indicating the various vetoing components.*

A detailed note on this problem should appear in the near future [12]. In the present work the LCAL was taken as an ideal veto but only for very energetic electrons (see section 6).

With a crossing angle, there are two blind regions of the vetoing device. One corresponds to the hole ($R = 1.2\,\mathrm{cm}$) needed for the entering beam, the other to the hole ($R = 1.2\,\mathrm{cm}$) needed for the exit of the disrupted beam. Both holes can also be surrounded with a vetoing device. Note also that due to the finite angle between the beam and the solenoidal field, the secondary electrons from the disrupted beam experience an azimuthally asymmetric curvature which also creates an asymmetric background distribution.

4 Generators and tools used for this analysis

The present analysis uses generators which were developed and tested at LEP2: SUSYGEN for the signal, BDKRC for the leptonic $\gamma\gamma$ background and Pythia including direct, VDM, anomalous and DIS sub-processes for the hadronic $\gamma\gamma$ background. The direct process stands for those interactions in which the bare photon interacts directly with its partner, the VDM for those where the photon fluctuates into a vector meson, predominantly ρ^0, the anomalous (or generalized VDM) in which the photon fluctuates into a $q\overline{q}$ pair of larger virtuality than in VDM process and the DIS corresponds to the deep inelastic scattering process $\gamma^* q \to q$ with q from the VDM and anomalous processes.

In addition to the previous processes with virtual photons one should take into account the processes due to real secondary photons induced by beamstrahlung. Figure 6 taken from [13] shows that these spectra, in the region of interest with photons between 1 and 10 GeV, increase the standard background by a factor of order 5. One should however note that contrary to virtual photons, the real-real spectrum has no transverse momentum and is therefore much less dangerous.

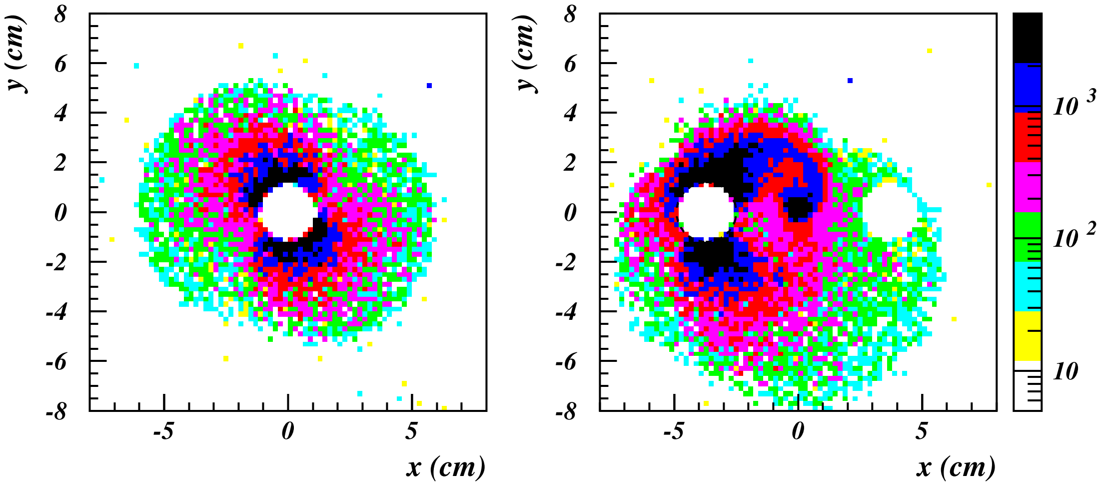

Figure 5: *Energy deposits in GeV from beamstrahlung in the TESLA configuration without and with crossing angle. Location is at* 3.7 m *downstream of the interaction point.*

Given the very large background cross sections involved, a procedure of enrichment was applied. A fast simulation program, SGV [14], was used since it provides a realistic and well tested simulation tool. This modelization was only used to define the acceptance of the detector for charged tracks and neutrals and to allow for secondary processes (e.g. conversion of photons) but no reconstruction effects were included (e.g. overlap of charged tracks and neutral deposits in the calorimeters).

The various points defined in section 2 were generated with emphasis on the most difficult ones which correspond to masses close to the energy threshold and with smallest mass difference between the slepton and the neutralino.

5 Analysis for the smuon channel

This channel is much easier to treat than the stau channel since, as shown in figure 7, the energy deposited by for smuons is much larger than for the lightest stau. This plot corresponds to the point D$'$ which has been selected as one of the most challenging ones.

The cuts used are the following (after applying the forward veto: two muons with transverse momentum greater than 2.5 GeV and with an azimuth difference below 160 degrees and an overall missing transverse momentum larger than 5 GeV. These cuts retain 80% of the signal. The results are shown in figure 7 for an integrated luminosity of 500 fb^{-1}. Both energy edges emerge cleanly above a small background which allows a very precise determination of the slepton and LSP masses. The latter will of course be used as an input to predict the amount of dark matter in the universe.

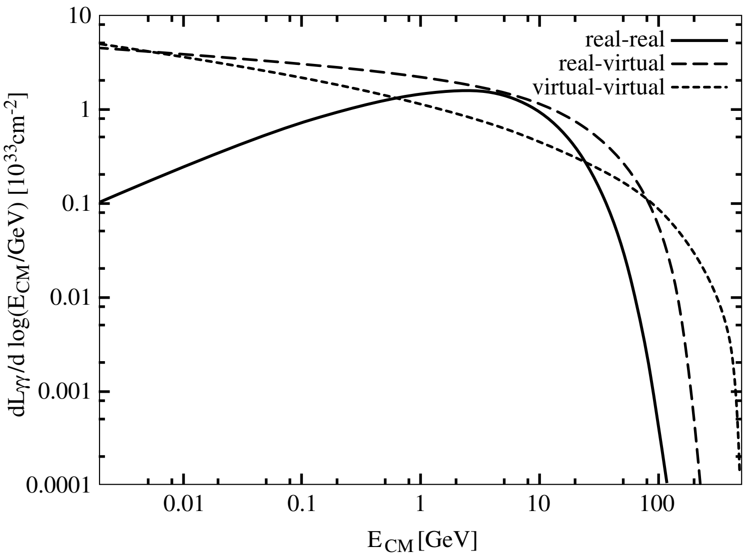

Figure 6: *Differential luminosity corresponding to the various components of $\gamma\gamma$ physics [13]. The so-called 'virtual-virtual' corresponds to the standard component induced by e^+e^- interaction. The two others correspond to interactions of real photons produced through beamstrahlung and which interact either with similar photons from the opposite beam (real-real) or with electrons/positrons from the opposite beam (real-virtual). In the energy domain of interest for this analysis, $\sim 10\,GeV$, one should multiply by 5 the rate due to the virtual-virtual contribution generated by our programs.*

6 Analysis for the stau channel

The working point chosen is D$'$ (see Table 1). This channel is primarily contaminated by $ee \to \tau\tau ee$ which will produce topologies similar to the signal. The process ee$\to$ $\mu\mu$ee can be suppressed, with a very small loss of efficiency, by vetoing final states with two identified muons.

In a small fraction of cases, however, such an event topology can occur where one of the spectator $e^\pm$ is emitted at relatively large angle and is misidentified as $\tau \to e\nu_e\nu_\tau$ decay while one of the real μ or τ goes to lower angles down to 20 mrad and cannot be detected by any detector unless the LAT (figure 4) has the capability of detecting a μ or π. For the present analysis, these background events are rejected by excluding eX topology. However, given the low analysis efficiency (table 3), it would be highly desirable to consider the possibility of providing an efficient μ/π identification in the forward instrumentation.

The WW background can also give a significant contribution to the stau analysis, via the $\tau\nu$ decay of the W. In practice the momentum and angular distributions of these τ particles behave differently from those of the signal which give very soft and isotropically distributed particles. Naïve selections leave only a few events and with a likelihood method (not implemented in the present analysis) one should essentially end up with a negligible background contribution (this would not of course be true for a large mass difference scenario).

A thorough investigation of the various hadronic sub-processes has also been carried out [15]. The dominant background comes from the process $ee \to c\bar{c}ee$, where one of the

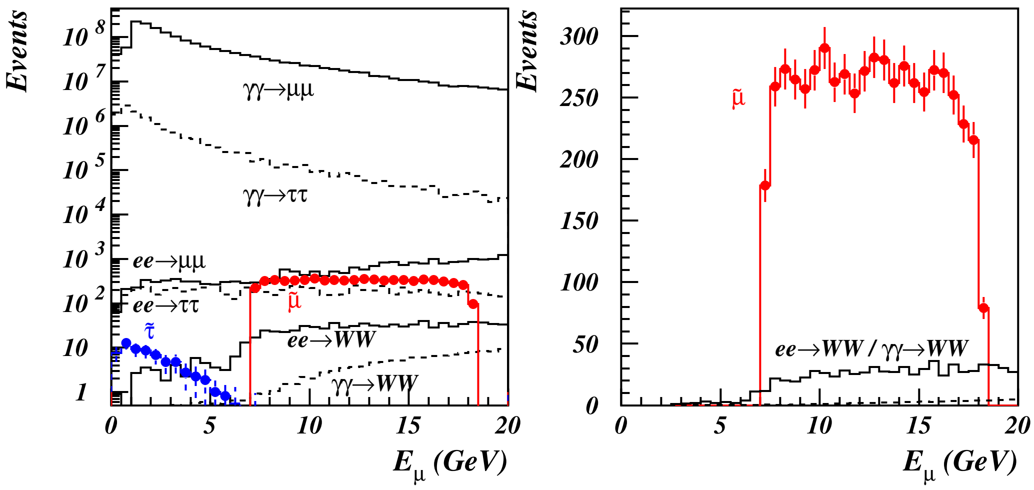

Figure 7: *The first plot shows the distribution of the muon energies of events selected with two muons. The second plot shows the same distribution after applying the cuts described in the smuon analysis.*

charm quarks decays semi-leptonically.

6.1 The leptonic background

The signal, as can be seen in figure 7, leaves a very small amount of visible energy as compared to the smuon analysis. The main selection relies on the fact that in the transverse plane the background τ leptons are back to back while they are uncorrelated in azimuth in the case of the signal. The crossing angle effect basically does not modify appreciably this situation when the final state electrons are properly vetoed. Using this feature, one can reconstruct the common direction of the τ particles by defining a thrust axis in the transverse plane. Then one computes ρ_T, the sum of the modules of the transverse momenta of individual particles with respect to this axis. The distribution of this quantity is displayed in figure 8, showing a clear separation between the $\tilde{\tau}$ signal and the $ee \to \tau\tau ee$ background.

The list of cuts given below is meant to remove both the leptonic and the hadronic backgrounds (e.g. veto on K_L^0 and neutrons):

1. veto on photons and electrons with a transverse momentum above 0.8 GeV and within 15 degrees with respect to the beam axis
2. request a $\tau^+\tau^-$ topology:
   - $1-1$, $1-3$, or $3-3$ prongs except for the eX and $\mu\mu$ topologies
   - if 3−prong, then no additional visible neutral particles
   - if there is a muon then only 1−prong and no additional visible neutral particles
   - no K_S^0, K_L^0 and neutron in the event

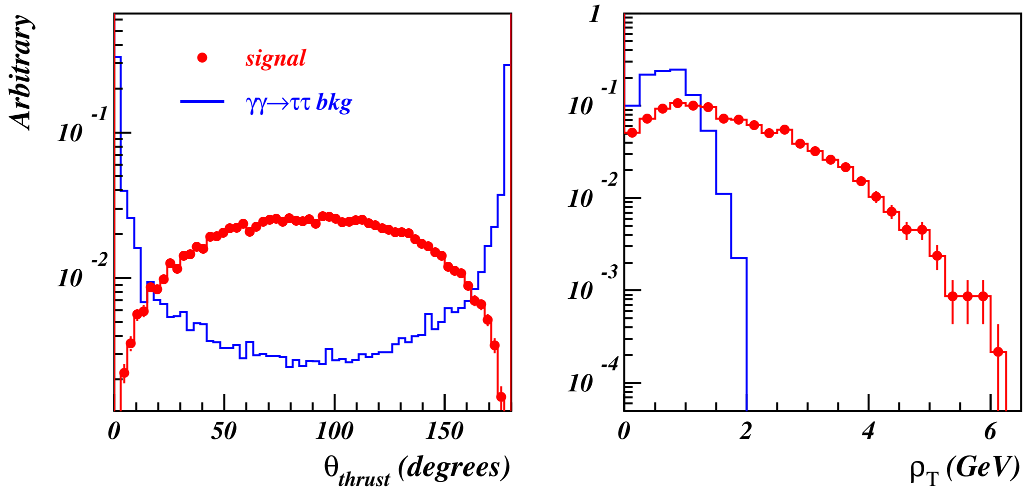

Figure 8: *The first plot shows the polar angle distribution of the thrust axis for the signal and for the background. Statistical fluctuations on background reflect the weighting procedure. The second plot shows the distribution for the variable ρ_T defined in the text and is obtained by adding all other cuts except the bi-dimensional cut shown in figure 11.*

- visible mass of the tau below 2 GeV
- correct charge in each hemisphere and total charge conserved

3. polar angle of the thrust axis (θ_{thrust}) between $15 - 165$ degrees and acoplanarity angle ($\phi_{Acoplanarity}$) below 145 degrees
4. maximum particle momentum below 15 GeV and the missing transverse momentum ($P_{T\,miss}$) of the event greater than 2.5 GeV
5. combined rejection on $\phi_{Acoplanarity}$ and ρ_T as indicated in figure 11.

In the case of a zero crossing angle and using the vetoing procedure defined in section 3, one remains with one tau background event with a weight of slightly below one and an efficiency of $6.3 \pm 0.2\%$ for $\sqrt{s} = 500$ GeV (table 2). This result does not depend significantly on the beam energy as was shown by generating the same sample at 442 GeV (table 3).

Table 2: *The efficiency, the signal and dominant background events in the head-on case for working point D' at $\sqrt{s} = 500$ GeV.*

Efficiency (%)	$N(\tilde{\tau} \to \tau\chi)$	$N(ee \to \tau\tau ee)$	$N(ee \to q\bar{q}ee)$ with $q = c, b$
6.3 ± 0.2	316 ± 9	1.0 ± 1.0	1.0 ± 1.0

The role of the efficiency veto is crucial as shown in figure 9. For angles above 0.5 degrees, one needs a rejection to better than a thousand while maintaining a fake rate at a reasonable level. Since the selection is applied not on energy but on transverse momentum one sees that for the smallest angles this veto is only requested for very energetic electrons, therefore easily recognized from the main background. As mentioned in section 3, there are ongoing studies to demonstrate the feasibility of this device.

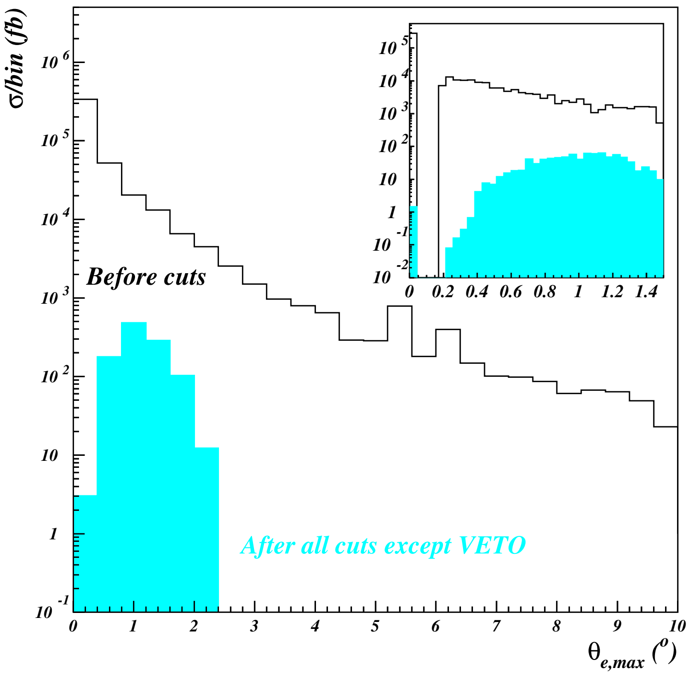

Figure 9: *Angular distribution of the spectator electrons from $ee \to \tau\tau ee$ expressed in fb/bin. The window shows the same distribution in the very forward region. In the inset, the peak at zero corresponds to those events where both electron and positron spectators stay in the beam-pipe. The light shaded distribution corresponds to the distribution obtained after all the selections described in the text, with the exception of the forward veto.*

In the case of a crossing angle, and without modifying above selection, one finds 4000 ± 225 events for the $ee \to \tau\tau ee$ background with a luminosity of $500\,\mathrm{fb}^{-1}$. The large majority of these events are easily identified as shown in the plot of figure 10. They are essentially due to events for which the final state electron/positron ends up in the 'wrong hole' i.e. in the entrance hole for the opposite beam. In such cases the $\gamma\gamma$ process will have an unbalanced transverse momentum of about 5 GeV pointing in the horizontal plane. This background can be almost entirely eliminated by a combined cut on $\phi_{Acoplanarity}$ and on the angle ($\phi_{PT\,miss}$) of the missing transverse momentum vector plane, as indicated in figure 11. There is then a relative reduction in efficiency of 25%.

How often does an electron end up in the wrong hole? This fraction depends on the size of the hole but is much larger than one would estimate on the basis of the solid angle. Typically one finds that the probability is 10^{-3}, which is certainly not negligible given

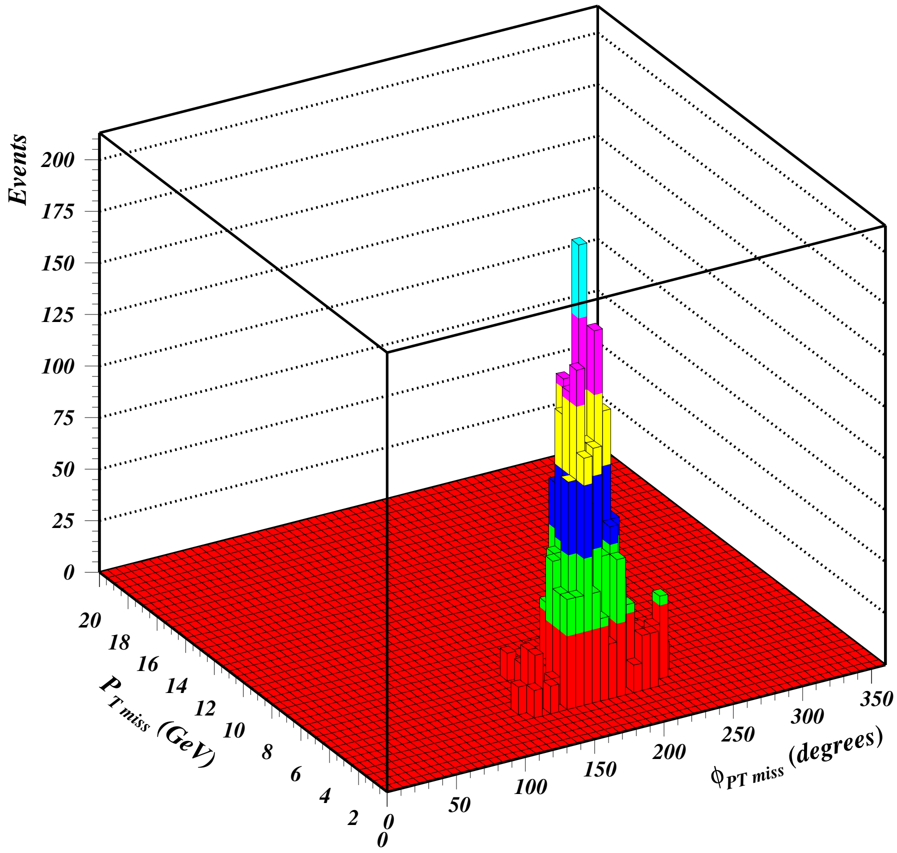

Figure 10: *Remaining $\gamma\gamma$ background events based on $ee \to \tau\tau ee$ with all cuts as for the head-on analysis. $P_{T\,miss}$ is the resulting transverse momentum of the visible particles, while $\phi_{PT\,miss}$ is the azimuthal orientation of this momentum.*

the rates.

Should one increase the energy to improve on the efficiency? Yes but in practice there could be no choice if there is a heavy $\tilde{\tau}_1$. Moreover, as pointed out in the next section, when the energy is increased one looses rapidly the sensitivity in determining the tau slepton mass.

6.2 The hadronic background

Hadronic sub-processes have an even larger cross sections but most have a topology distinct from the signal and, in particular do not produce appreciable missing transverse momenta. This feature appears clearly in figure 12 where the various hadronic sub-processes have been simulated [15] using Pythia. The major contribution comes from $ee \to c\bar{c}ee$ in direct on direct interactions, where the missing transverse momentum originates from the semi-leptonic decay of a charm particle. With the selections described in the preceding section one hadronic background event was left with an event weight of again slightly

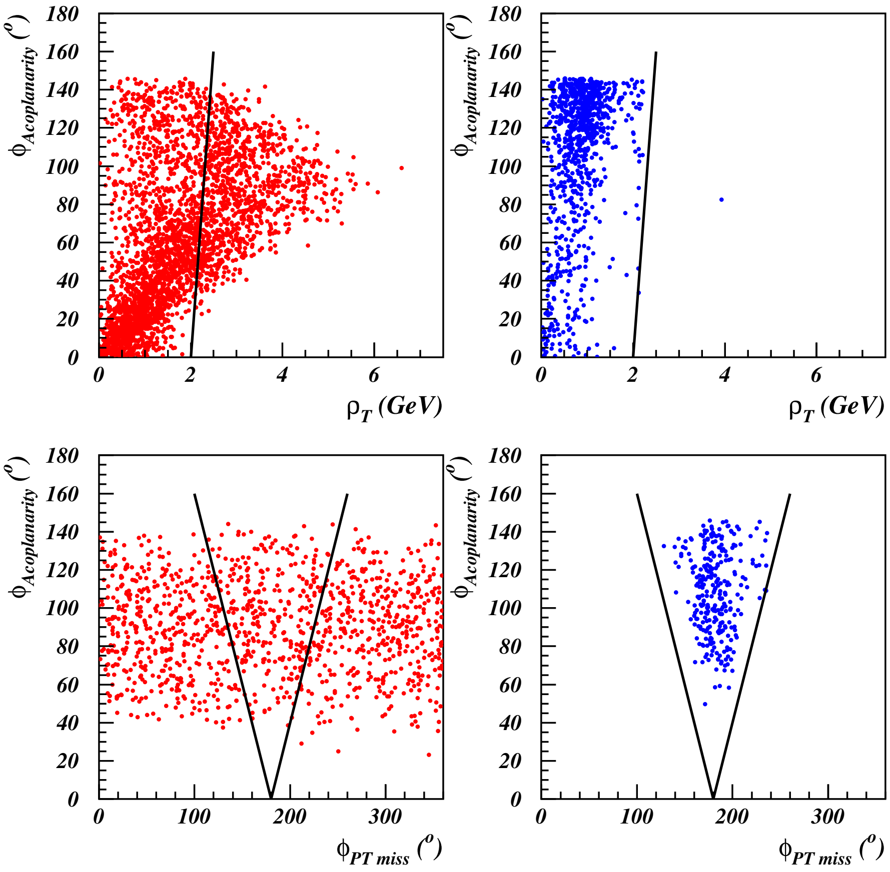

Figure 11: *Selections on the acoplanarity angle and on the ρ_T variables described in the text are displayed on top for the signal (in red, left plot) and on the background (in blue, right plot). Below are illustrated the variables used for the additional cuts needed with a crossing angle.*

below one (table 2).

6.3 Mini-jets

The influence of mini-jets is clearly machine dependent. In the case of TESLA, there is a 25 % probability to have a mini-jet with energy greater than 5 GeV per beam crossing. One therefore expects that in a few % of cases there could be two mini-jets superimposed. Such topologies are clearly not generated by standard codes and, for the present study, one can already attempt to crudely evaluate this contribution.

To do this, one generates mini-jet events and evaluates the probability p_τ that they produce a topology consistent with a single tau. One finds $p_\tau \sim 5 \cdot 10^{-4}$. Then one combines two such events occurring in the same crossing, with a probability of 3 % in the case of TESLA. Using the micro-vertex information, one eliminates mini-jets with inconsistent vertex. This keeps about 1 % of the events (3 times more in the case of

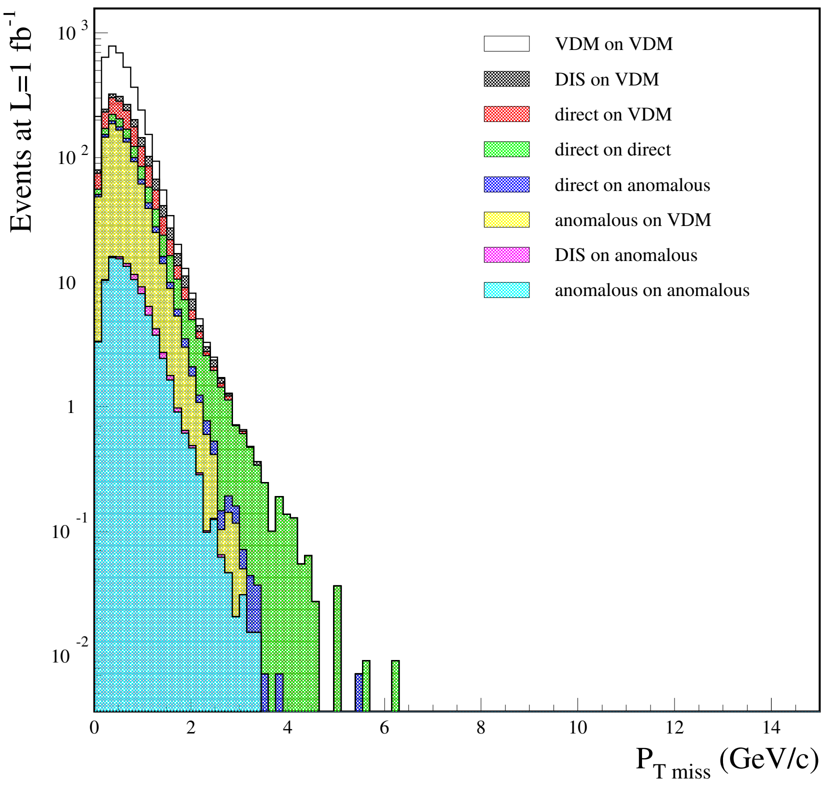

Figure 12: *Comparison of the different hadronic sub-processes indicating that the direct on direct process (green) gives the largest missing transverse momenta.*

a warm machine with a shorter bunch length). One applies the series of cuts defined previously which keeps about 10 % of these events. Finally one eliminates one half of the remaining events on the basis of charge conservation.

Taking into account the number of crossings corresponding to 500 fb^{-1}, one finds that this background gives about one event and therefore does not modify our overall conclusions. For the NLC technology the result depends on the number of bunches to be integrated. With a number of mini-jet/crossing 2.5 times smaller but with a bunch length 3 times shorter, NLC would give $\sim 0.5 N_b$ times the previous result, where N_b is the number of bunch within the time resolution which in our opinion should be at least 3.

6.4 Discussions

There are three caveats to the present studies:

- an ideal reconstruction and a perfect veto efficiency down to 3.2 mrad were assumed with a transverse momentum threshold at 0.8 GeV,
- only the dominant $\gamma\gamma$ background processes $\tau\tau$ and $q\bar{q}$ (with $q = c$ and b) were

studied with sufficient statistics,

- no effect of the machine backgrounds[4] were taken into account, in particular the overlapping mini-jets should also be considered since they could affect the reconstruction of the standard background and generate some tails in the distributions shown in figures 8 and 10.

With these caveats in mind, one concludes that in a LC even in this difficult case, clean $\tilde{\tau}$ samples with no significant background can be obtained and the mass of the lightest tau slepton can thus be determined (section 7.1). For the co-annihilation scenario, this result allows a model independent and precise prediction of the DM content of the universe.

7 Prediction of the DM content of the universe

In the co-annihilation scenario, the DM content of the universe depends primarily on two quantities:

- the mass of the LSP which can be determined, to a high accuracy, either using the chargino/neutralino or the smuon/selectron channel
- the mass of the lightest sleptons, and in particular the mass of the lightest stau which is determined with less precision.

These statements are general and do not assume any particular SUSY model like mSUGRA. In contrast, as was proposed in [16] for an LHC analysis, one assumed mSUGRA and extracted the scalar and gaugino masses from the cleanest observables (the smuon channel in the case of the LC). This approach, necessary at LHC, is clearly model dependent but, as shown in this paper, can be avoided in most cases in the LC environment.

7.1 Measurement of the stau mass using the threshold method

To extract the $\tilde{\tau}_1$ mass with minimum luminosity, the method consists in measuring the cross section at one energy and deduce the mass from the value of β since, at the Born level, this cross section depends on $\beta^3 = (1 - 4m^2/s)^{3/2}$, where m stands for the stau mass. One can also assume, as shown in figure 13, that the unpolarized cross section has very little dependence on the stau mixing angle which is true for reasonable values of the mixing angle, i.e. for a mixing angle below $\pi/4$. Above this value the lightest stau would be dominantly left-handed but this behavior is revealed with a polarized electron beam as shown in figure 13. This effect is so strong that with a sample of 50 events one could exclude such a possibility at the 6 s.d. level.

At which energy should one operate to achieve the best accuracy? One finds (see Appendix) that, without background and for a given integrated luminosity L (in fb^{-1}), the best accuracy is obtained very near threshold. The optimum is set by the requirement to observe a significant number of events, say at least $N > 10$ events. Then one finds that

[4] The machine background originating from beamstrahlung photons is, however, machine dependent (figure 6). The hadronic background is also subject to uncertainties on the cross section for hadron production in photon-photon collisions.

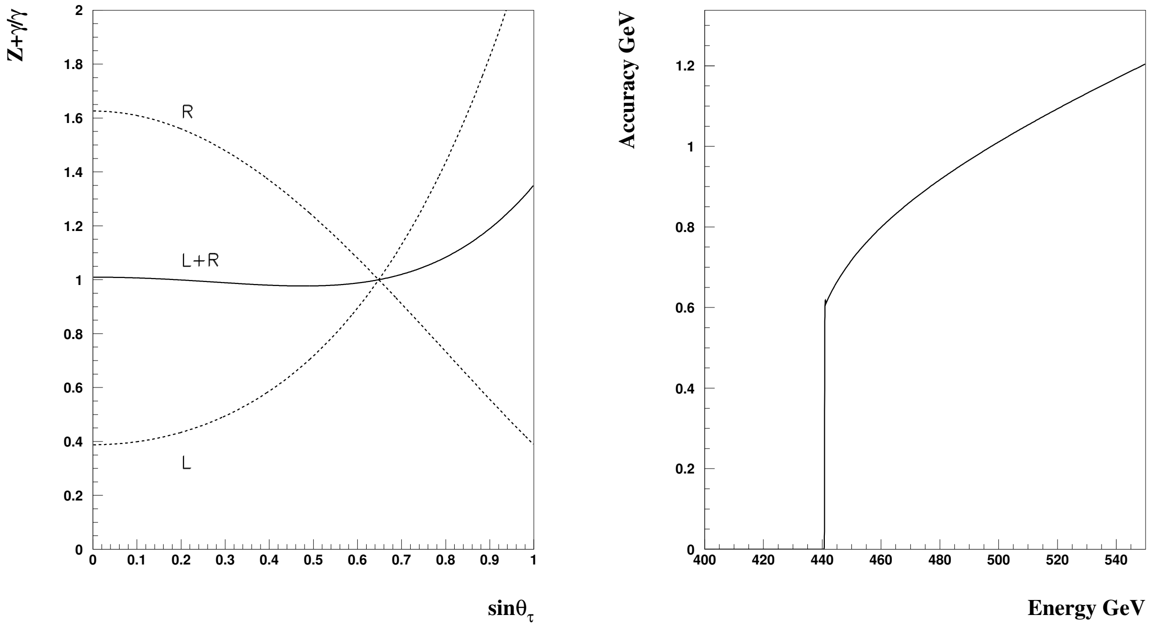

Figure 13: *The first plot gives the ratio between the stau cross sections, including the Z and the photon exchange and including only the photon exchange, versus the sine of the mixing angle in three cases: unpolarized beam (full line), right-handed electrons (dashed curved labeled R) and left-handed electrons (labeled L). The second plot gives the precision on the stau mass versus the center of mass energy for the working point D′. The cut near threshold reflects our choice to collect at least* 10 *events with* $500\,fb^{-1}$.

the optimum in energy is given by the condition $\beta^3 = N/(LA\epsilon)$ while the corresponding relative accuracy on the mass is given by:

$$\delta = \frac{(N)^{1/6}}{3(LA\epsilon)^{2/3}}\,.$$

where ϵ is the efficiency on the stau channel and A is a constant approximately equal to 100 fb at $\sqrt{s} = 500\,\mathrm{GeV}$ and varies like $1/s$. The above formula shows that there is a very slow dependence of the precision on the choice of N. If one requires 50 events instead of 10 to cross check the mixing hypothesis with polarized electrons, the same precision could be achieved by simply increasing the luminosity by 50%.

For point D′ this gives $\beta \simeq 0.19$ corresponding to a $\sim 0.5\,\mathrm{GeV}$ error on the stau mass for $500\,\mathrm{fb}^{-1}$ and an optimum $\sqrt{s}$ at $\sim 442\,\mathrm{GeV}$. The gain in luminosity with this choice is appreciable as can be seen in figure 13. Without optimization the error would have been 1.2 GeV.

Note that to achieve an optimum, one should have an a priori estimate of the stau mass and of the efficiency. This estimate can be guided by the results on the first two generation sleptons which also provide a determination of the LSP mass. For large value of $\tan\beta$, a precise estimate of the stau-LSP mass difference and therefore of the efficiency, could be delicate since, as can be seen in table 1, there can be large differences between the stau mass and the right-handed ordinary slepton masses. As previously mentioned in section 2, one could miss the smuon information in a scenario for which the first two generations are very heavy. In such cases, it is still possible to work out a strategy by first operating at the maximum energy to observe the stau signal and get a first estimate of the stau mass from the cross section which would allow to define the adequate center of mass energy for an optimal precision. For the LSP mass one should then use the chargino/neutralino reactions.

The simple formulae used for this discussion did not take into account ISR effects which are important for the stau cross section near threshold. It can be shown (see Appendix) that the effects on the stau cross section can be represented by a correction factor $0.86\beta^{2x}$ where x is the virtual radiator given by $x = 2\alpha/\pi[\log(s/m_e^2) - 1]$. As an example, this correction applied on point D′ gives a corrective factor of 0.53 for the optimized value $\beta \simeq 0.19$.

Results are summarized in table 3 for point D′ as well as for other relevant points assuming that $500\,\mathrm{fb}^{-1}$ has been taken at the optimized energies which are indicated. These results are obtained assuming that there is negligible background.

Table 3: *Error on the mass difference between the stau and the LSP with $500\,fb^{-1}$ luminosity (and an optimal choice of energy) for the TESLA assumptions. Effect on the relative uncertainty on $\Omega_{DM}h^2$.*

Model	A′	C′	D′	G′	J′
Optimal $\sqrt{s}$ GeV	505	337	442	316	700
Efficiency in %	10.4	14.3	5.7	14.4	< 1.0
Error on mass GeV	0.487	0.165	0.541	0.132	> 1.0
Error on $\Omega_{DM}h^2$ in %	3.4	1.8	6.9	1.6	> 14

In this discussion, one has ignored the energy spread of the effective luminosity which is machine dependent. This issue is common to various studies performed at the future LC (e.g. top threshold, SUSY thresholds) and precise methods are being developed to determine this differential luminosity based on e^+e^- scattering. The analysis described here is not more demanding in this respect than those developed e.g. for the top threshold. Thus the energy spread effects will not be investigated any further.

7.2 Determination of the SUSY DM component

The program Micromegas [17] has been used to compute the uncertainty on the DM density due to the SUSY mass error measurements. This program operates without any assumption, in particular it does not rely on the mSUGRA scheme.

Results are listed in table 3. It shows, as expected, that $\Omega_{DM}h^2$ depends primarily on the precision on the stau and LSP masses (through the Boltzmann law, as explained in the introduction). The present analysis, developed for the D′ solution, gives satisfactory results except for point J′ which is almost beyond detectability. It is however fair to say that no effort was invested to adapt this analysis for the J′ case. Points H′ and M′ are omitted since they do not pass the WMAP constraints within Micromegas. Points B′, E′, F′, I′, K′ and L′ are irrelevant since they have mass differences above 10 GeV and are easy to measure. One should notice that the point D′ itself, which corresponds to a negative value of μ, is marginally compatible with the $g-2$ result.

An alternative method, as previously noted, would be to work at the maximal energy of the collider and collect a large sample of events to analyze the high energy spectrum to estimate the mass of the stau. This could be done, with a 500 GeV collider, for point C′ and G′. It is however worth noting that the precision achieved with the threshold method is quite challenging and a comparison of the two methods should include systematic uncertainties.

7.3 A focus type solution

Table 4 gives the parameters of a 'focus' type solution taken from reference [4]. This solution predicts a light neutralino and the lightest chargino about 30 GeV heavier. One can therefore expect a clean signal and assume the mass accuracies given in [18]. One

Table 4: *Accuracies expected in the 'focus' scenario taken from [4].*

Parameters	$M1/2$	$m0$	$\tan\beta$	μ	m_{χ_1}	m_{χ_2}	$m_{\chi_1^\pm}$	$m_{\chi_2^\pm}$
Values (m, μ in GeV)	300	2500	30	121.6	85.6	135	113.1	274.8
Accuracies (m, μ in GeV)	–	–	$+25-11$	1.4	0.1	0.3	0.04	0.25
Error on $\Omega_{\rm DM}h^2$ in %	–	–	$+8.6-5.9$	$+2.9-2.1$	–	–	–	–

should be able to achieve threshold scans for the charginos and to access the mass difference through the dilepton mass distribution given by the $\chi_2\chi_1$ channel. One can then use the cross section measurement and the polarization asymmetry in the $\chi_1^+\chi_1^-$ channel to measure the parameter μ which governs the estimate of DM. This has been done assuming the accuracies given in [18] and the formulae taken from [19].

With these very precise chargino/neutralino masses, the main source of uncertainty is due to the cross section measurement and the main error on $\Omega_{\rm DM}h^2$ is due to $\tan\beta$ since there is a poor sensitivity for high values of $\tan\beta$. There is no other practical mean to determine this quantity, given that the sfermions and the heavy Higgses are inaccessible in the focus scenario. In spite of this, the precision achieved on $\Omega_{\rm DM}h^2$ would be largely sufficient to demonstrate a contradiction with the WMAP result and therefore imply that there are other sources of DM.

One therefore concludes that even if the observation of the chargino/neutralino sector is easy at a LC (and perhaps only achievable at a LC) in a focus scenario, the accuracy on the indirect determination of the DM content of the universe requires the highest possible accuracies. It is however fair to say that much more work is still needed to cover this scenario.

8 Conclusions

This analysis has shown that the detection and the mass measurement of the tau slepton, potentially important in view of the cosmological implications, is challenging in the so-called 'co-annihilation' scenario. A forward veto to remove the $\gamma\gamma$ background down to very small angles is essential to reach an almost background free result, adequate to achieve the accuracy implied by the post-WMAP generation in a model independent analysis.

From the present analysis, which includes the relevant backgrounds but not yet a fully realistic modelization of the detector response, one can already state that:

1. in the zero angle crossing situation, only possible in the TESLA scheme, the detection of the stau particles can be done with almost negligible background,

2. for these solutions, the requirement to match the Planck era precision demands luminosities of at least $500\,\mathrm{fb}^{-1}$ even with an optimized strategy of scanning. This further strengthens the need for a collider able to deliver the maximum luminosity, not necessarily at the maximum energy,

3. in the TESLA case, with a half crossing angle of 10 mrad, there is only a 25% degradation of the efficiency which therefore leaves open this possibility,

4. in the NLC case, the same conclusion could be reached provided that there is no degradation due to pile-up of several bunches in the forward veto (this may require some R&D for a very fast calorimeter).

Acknowledgements

Very useful contributions to the forward veto issue have been provided by K. Buesser, K. Moenig and A. Stahl. They are gratefully acknowledged. This study has also benefited from interesting suggestions and criticisms on the physics analysis aspects from G. Bélanger, U. Martyn, G.A. Moortgat-Pick and M. Peskin.

References

[1] M. Battaglia et al., *Eur. Phys. J.* **C33** (2004) 273-296, e-Print Archive: hep-ph/0306219.

[2] D. Hooper and T. Plehn, *Phys. Lett.* **B562** (2003) 18-27, e-Print Archive: hep-ph/0212226.

[3] R. Arnowitt et al., Aug. 2003, 13pp. e-Print Archive: hep-ph/0308159.

[4] H. Baer et al., *JHEP* **0402** (2004) 007, e-Print Archive: hep-ph/0311351.

[5] J. Ellis et al., *Phys. Lett.* **B573** (2003) 162-172, e-Print Archive: hep-ph/0305212.

[6] G.W. Bennett et al., (Muon $g-2$ Collaboration), Jan. 2004, e-Print Archive: hep-ex/0401008.

[7] E. De Lucia, Status of KLOE, 27th Meeting of the LNF Scientific Committee, 1st December 2003, http://www.lnf.infn.it/committee/27opensc.html.

[8] M. Davier, S. Eidelman, A. Hocker and Z. Zhang, *Eur. Phys. J.* **C31** (2003) 503-510, e-Print Archive: hep-ph/0308213.

[9] J. Ellis et al., Oct. 2003, e-Print Archive: hep-ph/0310356.

[10] D.E. Kaplan et al., *Phys. Rev.* **D 62** (2000) 035010, e-Print Archive: hep-ph/9911293; Z. Chacko et al., *JHEP* **001** (2000) 003, e-Print Archive: hep-ph/9911323.

[11] TESLA: Technical design report, part 4: A detector for TESLA, T. Behnke et al., DESY-2001-011, DESY-2001-011D, DESY-TESLA-2001-23, DESY-TESLA-FEL-2001-05, ECFA-2001-209, Mar. 2001.

[12] W. Lohmann et al., note to be published.

[13] This figure is taken from D. Schulte's thesis. Useful informations on his simulation program 'Guinea Pig' can be found in: http://www-sldnt.slac.stanford.edu/nlc/programs/guinea_pig/gp_index.html.

[14] SGV 2.31 - A fast and simple program for simulating high energy physics experiments at colliding beam detectors. http://b.home.cern.ch/b/berggren/www/sgv.html.

[15] M. Berggren, note to be published.

[16] G. Polesello, D.R. Tovey, Feb. 2004, e-Print Archive: hep-ph/0403047.

[17] G. Bélanger et al., *Comput. Phys. Commun.* **149** (2002) 103-120, e-Print Archive: hep-ph/0112278.

[18] TESLA: Technical design report, part 3: Physics at an e^+e^- linear collider, R.-D. Heuer et al., DESY-2001-011, DESY-TESLA-2001-23, DESY-TESLA-FEL-2001-05, ECFA-2001-209, Mar. 2001.

[19] S.Y. Choi et al., *Eur. Phys. J.* **C14** (2000) 535-546, e-Print Archive: hep-ph/0002033.

APPENDIX

1/ The ratio R=$\sigma/\sigma_{\gamma pointlike}$ for a stau is given by:

$$R = 0.215\beta^3[1 + (L+R)C_{\tilde{\tau}}/(1-K_Z) + (R^2+L^2)C_{\tilde{\tau}}^2/2(1-K_Z)^2]$$

with $K_Z = M_Z^2/s$, $s_W^2 \sim 0.21$, $L = (-0.5+s_W^2)/s_W c_W$, $R = s_W^2/s_W c_W$and $C_{\tilde{\tau}} = (-0.5s_{\tilde{\tau}}^2 + s_W^2)/c_W s_W$ where $s_{\tilde{\tau}}$ gives the mixing angle of the lightest stau (for $s_{\tilde{\tau}}$=0 one has a pure $\tilde{\tau_R}$). From above formula one deduces easily that for the weak or non mixing case one has:

$$R = 0.215\beta^3[1 - 0.1/(1-K_Z) + 0.1/(1-K_Z)^2]$$

which clearly shows that there is cancellation of the Z contribution (K_Z can be neglected at high energy). For maximum mixing, $s_{\tilde{\tau}}^2 = 0.5$, one has $C_{\tilde{\tau}} \sim 0$, which also gives a negligible Z contribution. This behavior is seen in figure 13.

With right-handed electrons, one has

$$R_R \sim 0.215\beta^3[1 + 1.03C_{\tilde{\tau}}/(1-K_Z) + 0.27C_{\tilde{\tau}}^2/(1-K_Z)^2]\,,$$

and with left-handed electrons:

$$R_L = 0.215\beta^3[1 - 1.42C_{\tilde{\tau}}/(1-K_Z) + 0.51C_{\tilde{\tau}}^2/(1-K_Z)^2]\,.$$

These two components behave very differently as can be seen in figure 13. One can therefore easily distinguish between a standard scenario where the lightest stau is dominantly right-handed for which there is no need to correct for mixing effects for the unpolarized cross section (or equivalently the average of the cross sections obtained with the two electron chiralities) and the opposite scenario for which a correction is needed if the LR asymmetry is of opposite sign and differs significantly from zero.

2/ The ISR effect can be treated simply using a soft photon approximation re-summed at all orders. One has the integral:

$$x\int_0^{th} u^{x-1}(\beta/\beta^0)^3 du$$

with $u = k/E$ where k is the photon energy, E the beam energy and where the integral is taken from 0 to the stau threshold. x is the effective radiator:

$$x = 2\alpha/\pi[\log(s/m_e^2) - 1]$$

with $x \sim 0.124$ at $\sqrt{s}$=500 GeV.

The effect is to replace β^3 in the stau cross section (p-wave dependence) by:

$$x\Gamma(x)\Gamma(5/2)\beta^{3+2x}/\Gamma(x+5/2)$$

which is $\sim 0.86\beta^{3+2x}$ at $\sqrt{s}$=500 GeV.

3/ To discuss in a simple way energy optimization for the stau mass determination, ISR corrections will be ignored. Given the efficiency ϵ, the luminosity L, and the cross section $\sigma = A\beta^3$, one can write the number of events produced as $N = LA\beta^3\epsilon$. The cross section depends on the stau mass through β and therefore one can simply translate the statistical error on N, $\sqrt{N}$, into a relative error on the mass δ through the formula:

$$\sqrt{N} = \sqrt{LA\beta^3\epsilon} = \frac{12m^2}{s} LA\epsilon\beta\delta\,.$$

One easily deduces that:

$$\delta = \frac{s}{12m^2}\sqrt{\frac{\beta}{LA\epsilon}}\,.$$

The dependence on s and β shows that, with all other parameters fixed, the precision improves when one operates near threshold. The limit of this optimum is set by the requirement to observe a significant number of events, say at least $N > 10$ events. Then one easily finds that the optimum in energy is given by the condition $\beta^3 = N/(LA\epsilon)$, while, from above formula, the accuracy is:

$$\delta = \frac{(N)^{1/6}}{3(LA\epsilon)^{2/3}}\,,$$

where the approximate relation $s = 4m^2$ near threshold has been applied. This formula illustrates two important features of the optimum method:

1. the relative precision on the mass has a weak dependence on the choice of N (going from 10 to 20 degrades δ by 12%)

2. the improvement in accuracy scales like $L^{2/3}$ and not like $L^{1/2}$ in the absence of an optimization.

The intuitive reason for the latter is that, with an increased luminosity and a fixed number of events, one can work at lower energy and therefore increase the sensitivity.

For point D′ this gives $\beta \simeq 0.19$ and a $\sim 0.5\,\mathrm{GeV}$ error on the stau mass for $500\,\mathrm{fb}^{-1}$ for an optimum energy $\sim 442\,\mathrm{GeV}$. The gain in luminosity with this optimal choice is appreciable. Without optimization, i.e. working at $\sqrt{s} = 500\,\mathrm{GeV}$, the error would have been $1.2\,\mathrm{GeV}$. Using the ISR corrected formulae one would find very similar results. No background was assumed in the above analysis.